ACS Partner Journal

CHEM & BIO ENGINEERING

pubs.acs.org/ChemBioEng

Article

A Solid-State Transformation of Hydrogen-Bonded Organic Frameworks for Efficient Acetylene Storage and Gas Separation

Published as part of Chem & Bio Engineering virtual special issue "Advanced Separation Materials and Processes".

Youlie Cai, Yanchun Zheng, Yiqi Chen, Runzhi Wei, Hui Xu,* and Junkuo Gao*

Cite This: *Chem Bio Eng.* 2024, 1, 615–622

Read Online

ACCESS | Metrics & More | Article Recommendations | Supporting Information

ABSTRACT: Developing robust microporous hydrogen-bonded organic frameworks (HOFs) is crucial for exploring novel physical adsorbents and revealing the structure–property relationship of hydrogen-bonding pairing behaviors. However, it is still challenging to obtain dense and stable hydrogen-bonded frameworks due to the rigidity and spatial resistance of the tectonic centers. Herein, we report a robust microporous HOF (HOF-ZSTU-4) via 4,4′,4′,4″-([1,1′-biphenyl]-4,4′-diylbis(azanetriyl))tetrabenzoic acid (H_4BDATB) with flexible nitrogen nodes composing the tectonic center. Single-crystal X-ray diffraction (SCXRD) analysis shows that the activated framework undergoes a solid-to-solid phase transition because of the torsion of the carboxyl–carboxyl dimer, leading to the switching of the framework from the *sql* topology to the *cds* topology (HOF-ZSTU-4a). The single-component gas sorption isotherm reveals that HOF-ZSTU-4a has a C_2H_2 packing density of 0.54 kg L^{-1}, marking it as the most efficient among reported HOFs. In addition, HOF-ZSTU-4a exhibits promising separation selectivity for several binary gas mixtures, and the dynamic separation performance for C_2H_2/CO_2, CO_2/N_2, and CH_4/N_2 is verified by dynamic breakthrough experiments.

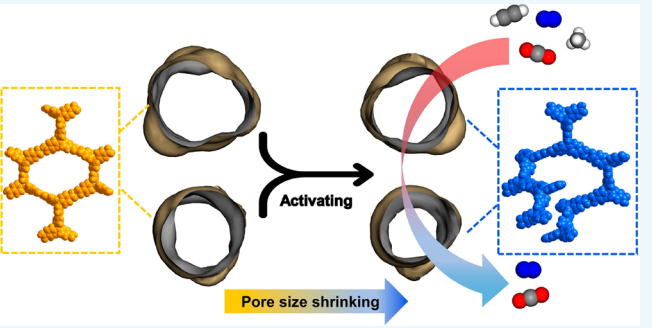

KEYWORDS: *acetylene storage, gas separation, hydrogen-bonded organic frameworks, micropores, solid–solid transitions*

INTRODUCTION

Porous materials have long been used for guest storage/separation and catalysis/transformation.[1−5] With the in-depth study of structure–property relationships, it has been difficult for traditional porous materials to meet a wide variety of modular structural designs. In the past few decades, several novel porous materials have been developed, including metal–organic frameworks (MOFs) and covalent organic frameworks (COFs).[6−13] Hydrogen-bonded organic frameworks (HOFs) are another newly developed class of porous materials, in which ordered hydrogen-bonded units are established through intermolecular hydrogen-bonding as well as several other interactions (e.g., $\pi\cdots\pi$ stacking, van der Waals forces, etc.).[14−25] The favorable solution processability and easy regeneration of HOFs have enabled their widespread interest in the field of gas separation.[26−30] With rationally designed hydrogen-bonding arm engineering, HOFs can also possess high surface area, high porosity, and expandable pore sizes.[31−35] The tectons with π-conjugated aromatic components allow the inherent good proton conductivity and biocompatibility of the assembled HOFs, thus HOFs are also widely used in optoelectronics,[36−38] carrier encapsulation,[39−41] and sensing.[42−45]

Concerning the rational design of HOFs with desired functionalities, the construction of HOFs with permanent porosity has been accomplished based on π-conjugated carboxylic acid tectons of porphyrins, pyrenes, polycycles, etc.[31,35,44,46−48] The rigid core and well-oriented hydrogen-bonded dimers make such HOFs feature high stability, high specific surface area, and high pore volume. However, the large pore size leads to insufficient confinement of gas molecules, making it difficult to be effective in critical gas separation. In addition, enhancing structural interpenetration alone is not sufficient for framework densification in most cases, e.g., the 3-fold interpenetrated ZJU-HOF-1,[49] the 5-fold interpenetrated HOF-TCBP and PFC-2,[31,50] and the 6-fold interpenetrated ZJU-HOF-10(sc) still exhibit large porosities.[51] Recent studies have shown that the tectons with nitrogen nodes exhibit flexible rotation to reduce the rigidity of the core and decrease

Received: November 29, 2023
Revised: January 15, 2024
Accepted: January 16, 2024
Published: February 1, 2024

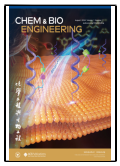

https://doi.org/10.1021/cbe.3c00100
Chem Bio Eng. 2024, 1, 615–622

the steric effects to achieve framework densification,[52−56] which is one of the options to build a robust three-dimensional (3D) HOF. Based on this, the introduction of multiple interpenetrations can enhance the multiple interactions and further improve the stability of HOFs.

Herein, we have successfully constructed a carboxylic acid HOF (HOF-ZSTU-4) based on 4,4′,4′,4″-([1,1′-biphenyl]-4,4′-diylbis(azanetriyl))tetrabenzoic acid (H_4BDATB), showing a 3D framework and a 5-fold interdigitated topology. Single-crystal X-ray diffraction (SCXRD) and powder X-ray diffraction (PXRD) analyses showed that activated HOF-ZSTU-4 (HOF-ZSTU-4a) undergoes a single-crystal to single-crystal transformation from the *sql* topology to the *cds* topology. The analysis of the single-crystal structure shows that the flexible deformation of the H_4BDATB molecule distorts the two hydrogen-bonding units in the symmetric position, leading to the transformation of the original lamellar hydrogen-bonding network into a helical structure. The close alignment of the two H_4BDATB molecules in the asymmetric unit causes the pores of the framework to shrink further, which arouses our interest in its use in gas separation. We investigated the potential of HOF-ZSTU-4a as an adsorbent for the selective separation of binary gas mixtures by single-component gas sorption isotherms. The dynamic breakthrough experimental results showed that HOF-ZSTU-4a could effectively separate binary mixtures of C_2H_2/CO_2, CO_2/N_2, and CH_4/N_2. In addition, HOF-ZSTU-4a can maintain its structure in some solvents and acid−base environments and has good thermal stability. This work presents a successful case of a solid-state phase transition from desolvation to generate a robust HOF.

RESULTS AND DISCUSSION

H_4BDATB (Figure S1) was sealed and held in a solution of acetic or propionic acid for 1 day at 150 °C until it cooled naturally to obtain pale green rod-like crystals of HOF-ZSTU-4 suitable for X-ray diffraction. SCXRD analysis showed that HOF-ZSTU-4 crystallizes in the $P\bar{1}$ space group and that the asymmetric unit consists of two intact H_4BDATB molecules. The hydrogen-bonding unit of HOF-ZSTU-4 is composed of carboxyl···carboxyl dimers. Considering H_4BDATB as a four-node scaffold, a basic ring of four tectons displays the *sql* topology (Figure 1 and Figure S2a). Two independent H_4BDATB molecules form a laminar network crossing in space at a plane angle of 54.2° to form a 5-fold interpenetrating 3D framework, and two types of one-dimensional (1D) pores distributed along the *a*-axis with sizes of 5.0 × 5.3 and 5.3 × 6.0 Å^2 are observed in the voids of the interpenetrating hydrogen-bonded layers.

The activated phase HOF-ZSTU-4a was obtained by degassing HOF-ZSTU-4. Besides, the activated phase could be obtained directly by volatilizing the methanol solution of H_4BDATB. Notably, the same PXRD spectra as those of HOF-ZSTU-4 were observed after immersing HOF-ZSTU-4a in acetic or propionic acid for 2 days, suggesting that the transition between the two is reversible (Figure S3). The SCXRD and PXRD results show that HOF-ZSTU-4a has different structural topological morphologies and diffraction peak positions, which suggests that the activated structure undergoes a solid−solid transition (Table S1). Compared to the synthesized sample, the cell volume of the activated structure shrinks from 3875 to 3602 Å^3, indicating a further densification of the structure. The cell α angle changed from 90.7° to 95.6° and the γ angle changed from 102.5° to 98.5°. These changes in the cell structure are attributed to rotation of the carboxyphenyl at the nitrogen node (Figures S4 and S5), causing distortion of the carboxyl···carboxyl dimer in the symmetric position (Figure 2a,b, Figure S6). In addition, the decrease in the dihedral angle of the central biphenyl further reduces the spatial resistance of the tecton (Figure S7). In contrast to the simplified four-membered ring of the synthesized sample, the activated structure extends rotationally in the form of a helical chain (Figure 2c). A stepped six-membered ring can be observed along the *b*-axis direction, showing a 9-fold interpenetrating *cds* topology (Figure 2d,e, Figure S2b). The 1D pore sizes along the *a*-axis direction shrink to 3.9 × 4.0 and 4.9 × 5.3 Å^2, respectively, which are more compatible with small molecule gases (Figure 2f,g).

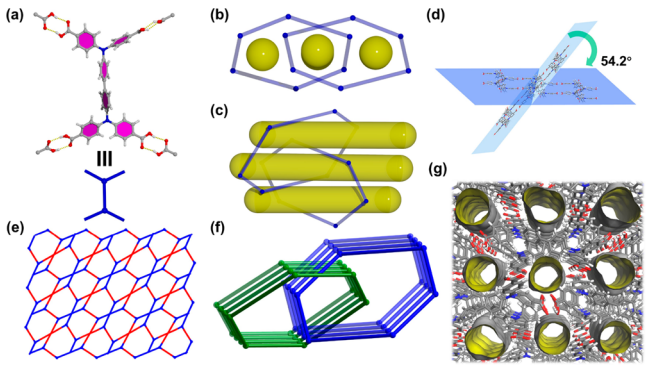

Figure 1. Crystal structure of HOF-ZSTU-4. (a) H_4BDATB as a four-node linked to four carboxyl groups from neighboring tectons. 1D pores are observed from the (b) *a*-axis and (c) *b*-axis, respectively, and are indicated by yellow columns. (d) Dihedral angles between interpenetrating planes. (e) Simplified demonstration diagram of the HOF-ZSTU-4 framework. (f) 5-fold interpenetration of the *sql* topology. (g) Diagram of 1D channel structure in the 3D model.

The structures of the synthesized and activated samples were determined by PXRD curves to agree with their respective crystal structures (Figure 3a). The activated samples have good crystallinity and can remain structurally stable in a range of chemical solvents, acid−base environments (pH = 2−12), and a wide temperature range (up to at least 180 °C) (Figure S8−S10). Scanning electron microscopy (SEM) revealed the morphology of HOF-ZSTU-4 as a micrometer-sized rod-like polyhedral structure (Figure S11). To determine the permanent porosity of HOF-ZSTU-4a, solvent exchange, vacuum-heated degassing, and supercritical carbon dioxide (sc-CO_2) drying methods were attempted for activating the pores of the samples, respectively, and the validity of the activation was verified by thermogravimetric analysis (TGA) (Figures S12 and S13). The pore properties of the activated samples were examined by sorption of N_2 at 77 K and CO_2 at 195 K (Figure 3b). HOF-ZSTU-4a showed a typical type-I sorption isotherm with uptake of 57 and 84 cm^3 g^{-1} for N_2 and CO_2, respectively, indicating permanent microporosity. The surface area calculated by the Brunauer−Emmett−Teller (BET) equation was 219 m^2 g^{-1} (Figure S14), which is close to the theoretical calculated value (215 m^2 g^{-1}). The Horvath−Kawazoe (H−K) microporous modeling analysis showed that the pore size of HOF-ZSTU-4a ranges from 4.0 to 5.6 Å (Figure S15). The pore volume was calculated to be 0.13 cm^3 g^{-1}, which agrees with the theoretical value (0.13 cm^3 g^{-1}).

https://doi.org/10.1021/cbe.3c00100
Chem Bio Eng. 2024, 1, 615−622

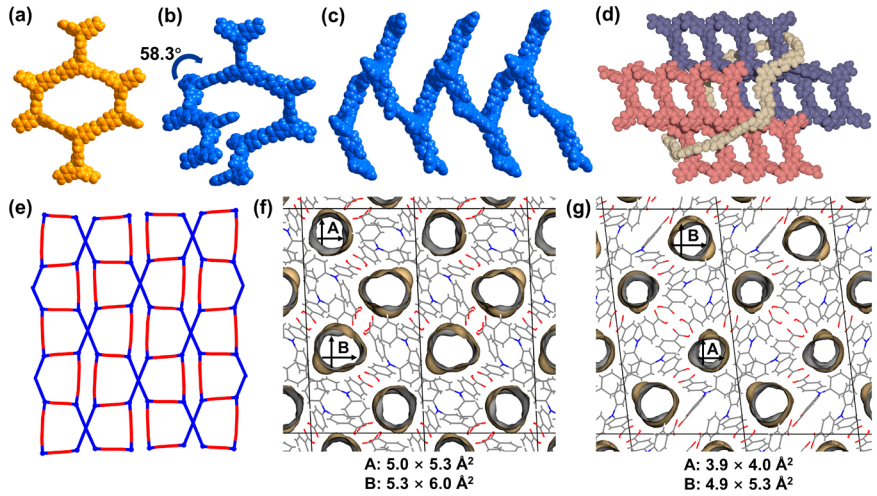

Figure 2. Crystal structure changes before and after activation. The changes in the four-membered ring before (a) and after (b) activation. (c) Demonstration of the rotational extension of the structure in the form of a helical chain after activation. (d) 9-fold interpenetration of the *cds* topology. (e) Simplified demonstration diagram of the HOF-ZSTU-4a framework. The apertures and dimensions of (f) HOF-ZSTU-4 and (g) HOF-ZSTU-4a.

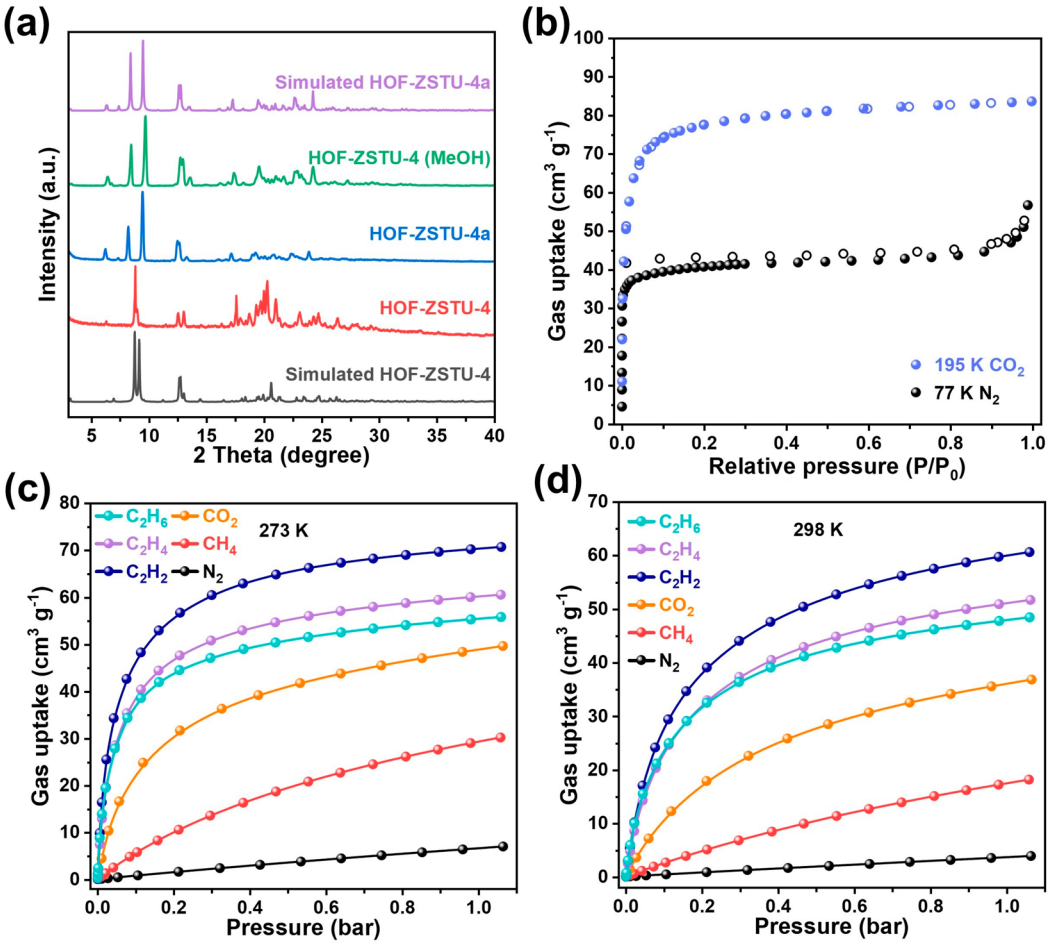

Figure 3. (a) Comparison of XRD curves of synthesized and activated samples with crystal structure simulations. (b) 77 K N_2 sorption isotherm and 195 K CO_2 sorption isotherm for HOF-ZSTU-4a. Single-component gas sorption isotherms at 273 K (c) and 298 K (d) for HOF-ZSTU-4a.

To evaluate the effect of HOF-ZSTU-4a on the adsorption of small molecule gases, the single-component gas sorption isotherm tests were carried out at 273 and 298 K (Figure 3c,d). The adsorption results showed that the adsorbed amounts of N_2, CH_4, CO_2, C_2H_2, C_2H_4, and C_2H_6 were 7.0, 30.2, 49.6, 70.7, 60.5, and 55.8 $cm^3\ g^{-1}$ at 273 K and 1 bar. When the temperature was increased to 298 K, the adsorbed amounts of each adsorbent decreased to 3.8, 18.2, 36.8, 60.6, 51.7, and 48.4 $cm^3\ g^{-1}$. Due to the relatively suitable pore size, the C_2H_2 uptake of HOF-ZSTU-4a was significantly higher than HOF-

https://doi.org/10.1021/cbe.3c00100
Chem Bio Eng. 2024, 1, 615−622

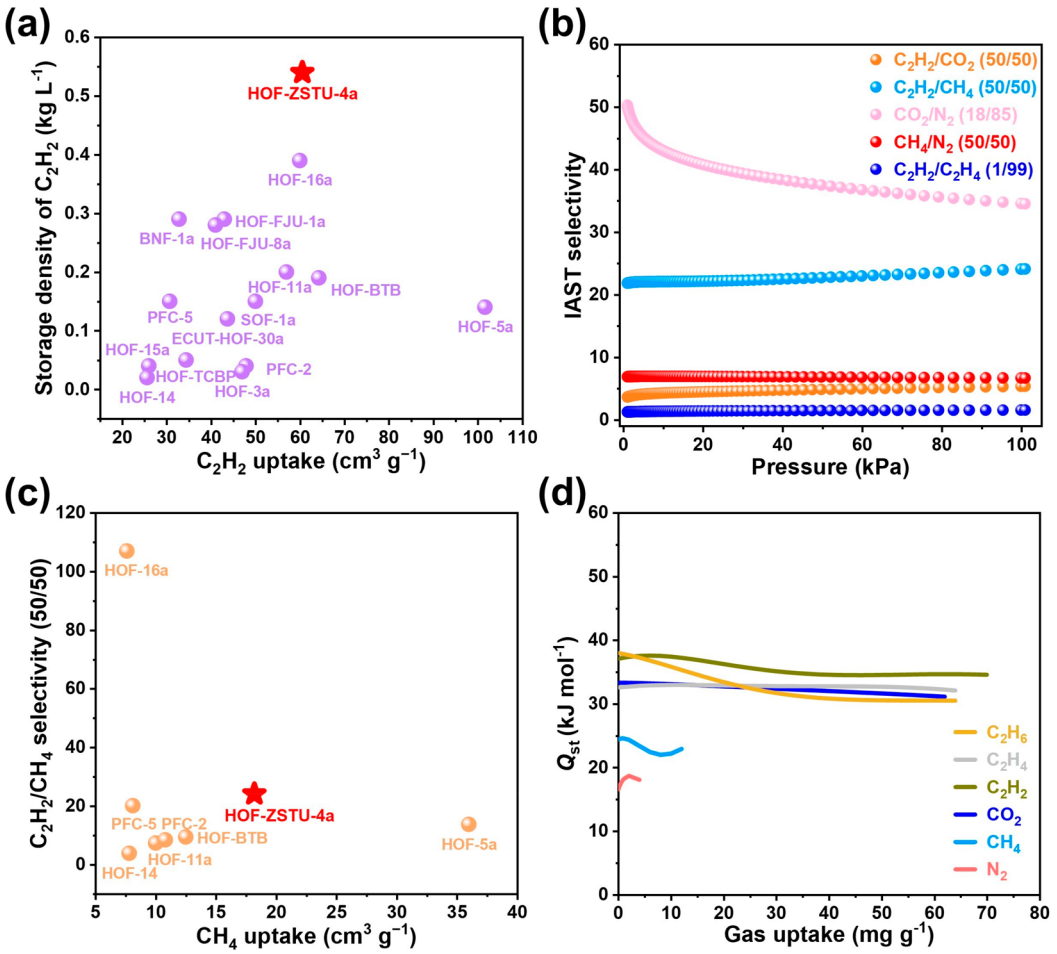

Figure 4. (a) C_2H_2 uptake and C_2H_2 packing density of HOF-ZSTU-4a compared with some other HOFs at 298 K and 1 bar. (b) Binary IAST selectivity for HOF-ZSTU-4a at 298 K. (c) CH_4 uptake and C_2H_2/CH_4 selectivity of HOF-ZSTU-4a compared with several HOFs at 298 K and 1 bar. (d) Isosteric heat of adsorption (Q_{st}) plots of gases on HOF-ZSTU-4a.

FJU-1a (43 cm^3 g^{-1}),[56] SOF-1a (50 cm^3 g^{-1}),[18] BNF-1a (32.8 cm^3 g^{-1}),[57] and HOF-3a (47 cm^3 g^{-1}),[58] which was comparable to HOF-16a (60 cm^3 g^{-1})[59] and HOF BTB (64.3 cm^3 g^{-1}) (Figure 4a).[60] Notably, several HOFs with larger pore sizes have low uptake due to insufficient confinement of C_2H_2 by the pore environment, e.g., HOF-TCBP (34.4 cm^3 g^{-1})[31] and PFC-2 (47.9 cm^3 g^{-1}).[50] The low pore volume and high C_2H_2 uptake of HOF-ZSTU-4a prompted us to investigate its storage performance for C_2H_2. At 298 K and 1 bar, the C_2H_2 packing density of HOF-ZSTU-4a reached 0.54 kg L^{-1}, which is significantly higher than previously reported HOFs and 1.4 times higher than the density of liquid C_2H_2 (0.393 kg L^{-1}) under the same conditions (Table S2),[61] suggesting that HOF-ZSTU-4a is a potential medium for C_2H_2 storage. Meanwhile, the excellent cyclic uptake capability of HOF-ZSTU-4a was verified by three consecutive C_2H_2 sorption−desorption tests at room temperature (Figure S16). Moreover, the uptake of CH_4 by HOF-ZSTU-4a was significantly higher than that of some related HOFs (Table S3), suggesting that the reduced pore size effectively traps CH_4, which is not common in HOFs constructed from purely organic components.

Ideal adsorbed solution theory (IAST) was used to evaluate the separation selectivity of the materials for some key gas mixtures (Figure 4b and Figure S17). At 298 K and 101 kPa, the IAST selectivity of HOF-ZSTU-4a for binary mixtures of C_2H_2/CO_2 (v/v = 50/50), C_2H_2/CH_4 (v/v = 50/50), CO_2/N_2 (v/v = 15/85), CH_4/N_2 (v/v = 50/50), and C_2H_2/C_2H_4 (v/v = 1/99) were 5.3, 24, 34.5, 6.6, and 1.5, respectively. The C_2H_2/CO_2 selectivity of HOF-ZSTU-4a was higher than HOF-16a (3.4) and HOF-FJU-8a (3.9),[54] comparable to BNF-1a (5.9). For C_2H_2/CH_4 mixtures, the selectivity is better than HOF-5a (13.6),[62] PFC-5 (20),[63] and HOF-BTB (9.3) (Figure 4c). In addition, the CO_2/N_2 selectivity of HOF-ZSTU-4a is also better than JLU-SOF2 (30) and JLU-SOF3 (22.8).[64] These results indicate that HOF-ZSTU-4a has potential applications in C_2H_2 purification, flue gas removal of CO_2, and natural gas upgrading. To assess the affinity of HOF-ZSTU-4a for adsorbates, the isosteric heat of adsorption (Q_{st}) was calculated based on the single-component sorption isotherms at 273 and 298 K (Figure 4d and Figure S18). The Q_{st} values for N_2, CH_4, CO_2, C_2H_2, C_2H_4, and C_2H_6 at zero coverage were 16.5, 24.4, 33.3, 37.0, 32.5, and 37.9 kJ mol^{-1}, suggesting that HOF-ZSTU-4a has a moderate affinity for gas molecules, while providing low-energy desorption of gases.

The adsorption profiles of C_2H_2, CO_2, and CH_4 were investigated via GCMC simulations. The simulation results show that C_2H_2 preferentially binds in a lateral mode in pore B of HOF-ZSTU-4a, with the head and tail each forming a moderately strong C−H···O interaction with a carboxylate oxygen on the pore wall at distances of 3.238 and 3.319 Å

https://doi.org/10.1021/cbe.3c00100
Chem Bio Eng. 2024, 1, 615−622

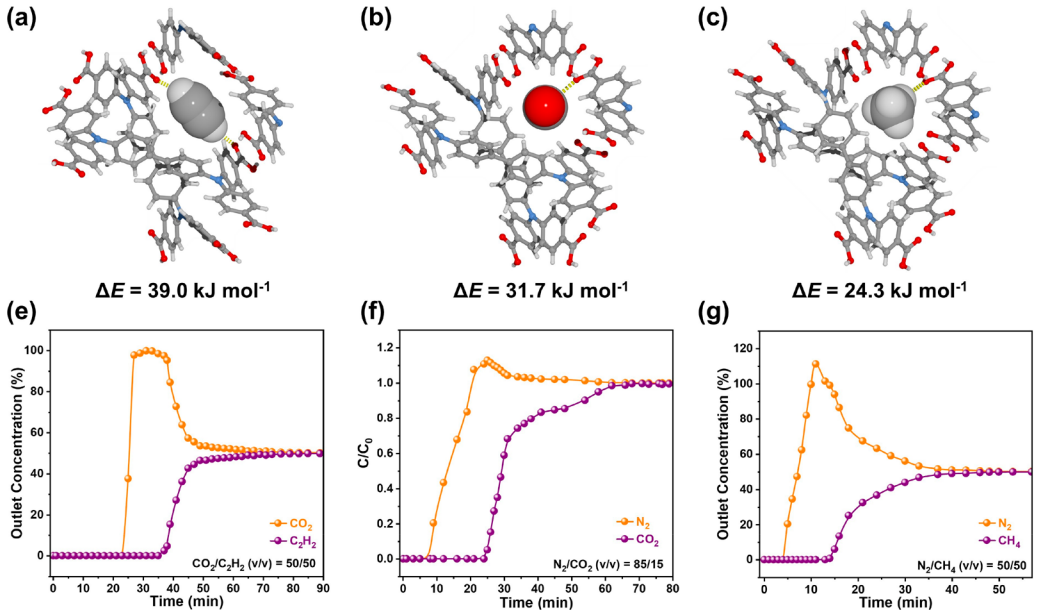

Figure 5. (a) Preferential binding site for C_2H_2 molecules in pore B of HOF-ZSTU-4a. Preferential binding sites for (b) the CO_2 and (c) the CH_4 molecules in pore A of HOF-ZSTU-4a. Dynamic breakthrough curves of (e) C_2H_2/CO_2 (v/v = 50/50), (f) CO_2/N_2 (v/v = 15/85), and (g) CH_4/N_2 (v/v = 50/50) under ambient conditions.

(Figure 5a). For both CO_2 and CH_4 molecules, the preferential binding sites are located at the smaller size of pore A, in a vertical binding mode forming a C−H···O interaction with a carboxylate group at distances of 3.137 and 3.432 Å (Figure 5b,c). The static binding energies obtained from the simulations are 39, 31.7, and 24.3 kJ mol^{-1}, respectively, which are in better agreement with the experimental values. The distribution of gas molecules inside the pore channel is revealed by density distribution maps (Figure S19). At 298 K and 101 kPa, both CO_2 and CH_4 are continuously distributed in pore B, while the distribution in pore A is discrete, which is attributed to the smaller pore size. In contrast, the lateral binding mode of C_2H_2 in pore B and the larger window size of pore B led to contrary distribution behavior. The per cell loadings of C_2H_2, CO_2, and CH_4 obtained from GCMC simulations were 6.9, 4.3, and 2.8, respectively, corresponding to uptake of 59.4, 36.3, and 20.7 $cm^3\ g^{-1}$, which were close to the experimental values.

The separation performance of HOF-ZSTU-4a for binary mixtures of C_2H_2/CO_2 (v/v = 50/50), CO_2/N_2 (v/v = 15/85), and CH_4/N_2 (v/v = 50/50) was further verified by dynamic breakthrough tests. As shown in Figure 5e, when the C_2H_2/CO_2 mixture was passed through the filled column, CO_2 was first detected at 23 min, while C_2H_2 did not break through until it reached adsorption saturation at 35 min. For the CO_2/N_2 mixture, the retention times of N_2 and CO_2 were 5 and 24 min (Figure 5f); for the CH_4/N_2 mixture, the retention times of N_2 and CH_4 were 4 and 13 min (Figure 5g). The separation time intervals of the two components in the mixtures reached 12, 19, and 9 min, respectively, which indicated that HOF-ZSTU-4a exhibited efficient separation performance in all three mixtures. The total dynamic uptake of HOF-ZSTU-4a during mixture separation was calculated to be 9.1 (for C_2H_2/CO_2 mixtures), 7.5 (for CO_2/N_2 mixtures), and 4.0 L/kg (for CH_4/N_2 mixtures), with dynamic separation selectivities of 4.7, 2.8, and 6.9, respectively.

CONCLUSIONS

In conclusion, a carboxylic-acid-based microporous HOF undergoing a solid−solid transition after activation was constructed by utilizing the flexibility of the nitrogen nodes to reduce the spatial resistance between the tectons. SCXRD analysis has revealed a 3D topological reconstruction, prompted by the flexible deformation of the tectons, resulting in a contracted pore size. The excellent stability of the structure-transformed HOF is demonstrated by a series of stability experiments. Moreover, the activated HOF demonstrated efficient separation performance for gas mixtures such as such as C_2H_2/CO_2, CO_2/N_2, and CH_4/N_2, as evidenced by both static gas adsorption experiments and dynamic breakthrough tests. Theoretical calculations have provided insight into the potential adsorption sites. This study not only sheds light on the structure−property relationships following structural transformations in HOFs but also sets the stage for future explorations of the design of HOFs with tailored properties for specific applications.

ASSOCIATED CONTENT

Supporting Information

The Supporting Information is available free of charge at https://pubs.acs.org/doi/10.1021/cbe.3c00100.

CIF file for HOF-4 (CIF)

CIF file for HOF-4a (CIF)

Experimental details and calculations; diagram of the molecular structure, topology diagrams, PXRD patterns, torsion angles, dihedral angles, gas adsorption and desorption isotherms, SEM images, TGA curves, BET surface area plot, pore size distribution, sorption−desorption curves, fitting results, density profiles; tables of crystal data and adsorption data (PDF)

Accession Codes

CCDC (2311097-2311098) contains the supplementary crystallographic data for this paper. These data can be

https://doi.org/10.1021/cbe.3c00100
Chem Bio Eng. 2024, 1, 615−622

obtained free of charge via www.ccdc.cam.ac.uk/data_request/cif, or by emailing data_request@ccdc.cam.ac.uk, or by contacting The Cambridge Crystallographic Data Centre, 12 Union Road, Cambridge CB2 1EZ, UK; fax: +44 1223 336033.

AUTHOR INFORMATION

Corresponding Authors

Hui Xu − *Institute of Optoelectronic Materials and Devices, China Jiliang University, Hangzhou 310018, China*; Email: huixu@cjlu.edu.cn

Junkuo Gao − *School of Materials Science and Engineering, Zhejiang Sci-Tech University, Hangzhou 310018, China*; orcid.org/0000-0001-9778-4312; Email: jkgao@zstu.edu.cn

Authors

Youlie Cai − *School of Materials Science and Engineering, Zhejiang Sci-Tech University, Hangzhou 310018, China*; orcid.org/0000-0003-3092-1452

Yanchun Zheng − *School of Materials Science and Engineering, Zhejiang Sci-Tech University, Hangzhou 310018, China*

Yiqi Chen − *School of Materials Science and Engineering, Zhejiang Sci-Tech University, Hangzhou 310018, China*

Runzhi Wei − *School of Materials Science and Engineering, Zhejiang Sci-Tech University, Hangzhou 310018, China*

Complete contact information is available at: https://pubs.acs.org/10.1021/cbe.3c00100

Notes

The authors declare no competing financial interest.

ACKNOWLEDGMENTS

This work was supported by the National Natural Science Foundation of China (No. 22378366).

REFERENCES

(1) Slater, A. G.; Cooper, A. I. Function-led design of new porous materials. *Science* **2015**, *348* (6238), No. aaa8075.

(2) Ben, T.; Ren, H.; Ma, S.; Cao, D.; Lan, J.; Jing, X.; Wang, W.; Xu, J.; Deng, F.; Simmons, J. M.; et al. Targeted Synthesis of a Porous Aromatic Framework with High Stability and Exceptionally High Surface Area. *Angew. Chem. Int. Ed.* **2009**, *48* (50), 9457−9460.

(3) Li, H.; Eddaoudi, M.; Groy, T. L.; Yaghi, O. M. Establishing Microporosity in Open Metal−Organic Frameworks: Gas Sorption Isotherms for Zn(BDC) (BDC = 1,4-Benzenedicarboxylate). *J. Am. Chem. Soc.* **1998**, *120* (33), 8571−8572.

(4) Jiang, H.-L.; Liu, B.; Lan, Y.-Q.; Kuratani, K.; Akita, T.; Shioyama, H.; Zong, F.; Xu, Q. From Metal−Organic Framework to Nanoporous Carbon: Toward a Very High Surface Area and Hydrogen Uptake. *J. Am. Chem. Soc.* **2011**, *133* (31), 11854−11857.

(5) Lin, R.-B.; He, Y.; Li, P.; Wang, H.; Zhou, W.; Chen, B. Multifunctional porous hydrogen-bonded organic framework materials. *Chem. Soc. Rev.* **2019**, *48* (5), 1362−1389.

(6) Yaghi, O. M.; Li, G.; Li, H. Selective binding and removal of guests in a microporous metal−organic framework. *Nature* **1995**, *378* (6558), 703−706.

(7) Côté, A. P.; Benin, A. I.; Ockwig, N. W.; O'Keeffe, M.; Matzger, A. J.; Yaghi, O. M. Porous, Crystalline, Covalent Organic Frameworks. *Science* **2005**, *310* (5751), 1166−1170.

(8) Kondo, M.; Yoshitomi, T.; Matsuzaka, H.; Kitagawa, S.; Seki, K. Three-Dimensional Framework with Channeling Cavities for Small Molecules: {[M_2(4, 4′-bpy)$_3$(NO_3)$_4$]·xH_2O}n (M=Co, Ni, Zn). *Angew. Chem. Int. Ed.* **1997**, *36* (16), 1725−1727.

(9) Zhang, C.-R.; Cui, W.-R.; Yi, S.-M.; Niu, C.-P.; Liang, R.-P.; Qi, J.-X.; Chen, X.-J.; Jiang, W.; Liu, X.; Luo, Q.-X.; et al. An ionic vinylene-linked three-dimensional covalent organic framework for selective and efficient trapping of ReO_4^- or $^{99}TcO_4^-$. *Nat. Commun.* **2022**, *13* (1), 7621.

(10) Liu, T.; Zhao, Y.; Song, M.; Pang, X.; Shi, X.; Jia, J.; Chi, L.; Lu, G. Ordered Macro−Microporous Single Crystals of Covalent Organic Frameworks with Efficient Sorption of Iodine. *J. Am. Chem. Soc.* **2023**, *145* (4), 2544−2552.

(11) Xu, H.; Tao, S.; Jiang, D. Proton conduction in crystalline and porous covalent organic frameworks. *Nat. Mater.* **2016**, *15* (7), 722−726.

(12) Kang, F.; Wang, X.; Chen, C.; Lee, C.-S.; Han, Y.; Zhang, Q. Construction of Crystalline Nitrone-Linked Covalent Organic Frameworks Via Kröhnke Oxidation. *J. Am. Chem. Soc.* **2023**, *145* (28), 15465−15472.

(13) Sun, J.; Xu, Y.; Lv, Y.; Zhang, Q.; Zhou, X. Recent Advances in Covalent Organic Framework Electrode Materials for Alkali Metal-Ion Batteries. *CCS Chem.* **2023**, *5* (6), 1259−1276.

(14) Ermer, O. Five-fold diamond structure of adamantane-1,3,5,7-tetracarboxylic acid. *J. Am. Chem. Soc.* **1988**, *110* (12), 3747−3754.

(15) Simard, M.; Su, D.; Wuest, J. D. Use of hydrogen bonds to control molecular aggregation. Self-assembly of three-dimensional networks with large chambers. *J. Am. Chem. Soc.* **1991**, *113* (12), 4696−4698.

(16) Hisaki, I.; Xin, C.; Takahashi, K.; Nakamura, T. Designing Hydrogen-Bonded Organic Frameworks (HOFs) with Permanent Porosity. *Angew. Chem. Int. Ed.* **2019**, *58* (33), 11160−11170.

(17) Venkataraman, D.; Lee, S.; Zhang, J.; Moore, J. S. An organic solid with wide channels based on hydrogen bonding between macrocycles. *Nature* **1994**, *371* (6498), 591−593.

(18) Yang, W.; Greenaway, A.; Lin, X.; Matsuda, R.; Blake, A. J.; Wilson, C.; Lewis, W.; Hubberstey, P.; Kitagawa, S.; Champness, N. R.; et al. Exceptional Thermal Stability in a Supramolecular Organic Framework: Porosity and Gas Storage. *J. Am. Chem. Soc.* **2010**, *132* (41), 14457−14469.

(19) He, Y.; Xiang, S.; Chen, B. A Microporous Hydrogen-Bonded Organic Framework for Highly Selective C_2H_2/C_2H_4 Separation at Ambient Temperature. *J. Am. Chem. Soc.* **2011**, *133* (37), 14570−14573.

(20) Wang, B.; Lin, R.-B.; Zhang, Z.; Xiang, S.; Chen, B. Hydrogen-Bonded Organic Frameworks as a Tunable Platform for Functional Materials. *J. Am. Chem. Soc.* **2020**, *142* (34), 14399−14416.

(21) Li, P.; Ryder, M. R.; Stoddart, J. F. Hydrogen-Bonded Organic Frameworks: A Rising Class of Porous Molecular Materials. *Acc. Mater. Res.* **2020**, *1* (1), 77−87.

(22) Yamagishi, H.; Sato, H.; Hori, A.; Sato, Y.; Matsuda, R.; Kato, K.; Aida, T. Self-assembly of lattices with high structural complexity from a geometrically simple molecule. *Science* **2018**, *361* (6408), 1242−1246.

(23) Ma, K.; Li, P.; Xin, J. H.; Chen, Y.; Chen, Z.; Goswami, S.; Liu, X.; Kato, S.; Chen, H.; Zhang, X.; et al. Ultrastable Mesoporous Hydrogen-Bonded Organic Framework-Based Fiber Composites toward Mustard Gas Detoxification. *Cell Rep. Phys. Sci.* **2020**, *1* (2), No. 100024.

(24) Deng, J.-H.; Luo, J.; Mao, Y.-L.; Lai, S.; Gong, Y.-N.; Zhong, D.-C.; Lu, T.-B. π-π stacking interactions: Non-negligible forces for stabilizing porous supramolecular frameworks. *Sci. Adv.* **2020**, *6* (2), No. eaax9976.

(25) Zhang, C.; Li, Y.; Yu, F.; Wang, G.; Wang, K.; Ma, C.; Yang, X.; Zhou, Y.; Zhang, Q. Visual growth of nano-HOFs for low-power memristive spiking neuromorphic system. *Nano Energy* **2023**, *109*, No. 108274.

(26) Luo, X.-Z.; Jia, X.-J.; Deng, J.-H.; Zhong, J.-L.; Liu, H.-J.; Wang, K.-J.; Zhong, D.-C. A Microporous Hydrogen-Bonded Organic Framework: Exceptional Stability and Highly Selective Adsorption of Gas and Liquid. *J. Am. Chem. Soc.* **2013**, *135* (32), 11684−11687.

(27) Das, M. C.; Pal, S. C.; Chen, B. Emerging microporous HOF materials to address global energy challenges. *Joule* **2022**, *6* (1), 22−27.
(28) Xi, X.-J.; Li, Y.; Lang, F.-F.; Xu, L.; Pang, J.; Bu, X.-H. Robust porous hydrogen-bonded organic frameworks: Synthesis and applications in gas adsorption and separation. *Giant* **2023**, *16*, No. 100181.
(29) Yang, Y.; Li, L.; Lin, R.-B.; Ye, Y.; Yao, Z.; Yang, L.; Xiang, F.; Chen, S.; Zhang, Z.; Xiang, S.; et al. Ethylene/ethane separation in a stable hydrogen-bonded organic framework through a gating mechanism. *Nat. Chem.* **2021**, *13* (10), 933−939.
(30) Cai, Y.; Gao, J.; Li, J.-H.; Liu, P.; Zheng, Y.; Zhou, W.; Wu, H.; Li, L.; Lin, R.-B.; Chen, B. Pore Modulation of Hydrogen-Bonded Organic Frameworks for Efficient Separation of Propylene. *Angew. Chem. Int. Ed.* **2023**, *62* (37), No. e202308579.
(31) Hu, F.; Liu, C.; Wu, M.; Pang, J.; Jiang, F.; Yuan, D.; Hong, M. An Ultrastable and Easily Regenerated Hydrogen-Bonded Organic Molecular Framework with Permanent Porosity. *Angew. Chem. Int. Ed.* **2017**, *56* (8), 2101−2104.
(32) Suzuki, Y.; Gutiérrez, M.; Tanaka, S.; Gomez, E.; Tohnai, N.; Yasuda, N.; Matubayasi, N.; Douhal, A.; Hisaki, I. Construction of isostructural hydrogen-bonded organic frameworks: limitations and possibilities of pore expansion. *Chem. Sci.* **2021**, *12* (28), 9607−9618.
(33) Song, X.; Wang, Y.; Wang, C.; Wang, D.; Zhuang, G.; Kirlikovali, K. O.; Li, P.; Farha, O. K. Design Rules of Hydrogen-Bonded Organic Frameworks with High Chemical and Thermal Stabilities. *J. Am. Chem. Soc.* **2022**, *144* (24), 10663−10687.
(34) Hisaki, I.; Suzuki, Y.; Gomez, E.; Cohen, B.; Tohnai, N.; Douhal, A. Docking Strategy To Construct Thermostable, Single-Crystalline, Hydrogen-Bonded Organic Framework with High Surface Area. *Angew. Chem. Int. Ed.* **2018**, *57* (39), 12650−12655.
(35) Yin, Q.; Zhao, P.; Sa, R.-J.; Chen, G.-C.; Lü, J.; Liu, T.-F.; Cao, R. An Ultra-Robust and Crystalline Redeemable Hydrogen-Bonded Organic Framework for Synergistic Chemo-Photodynamic Therapy. *Angew. Chem. Int. Ed.* **2018**, *57* (26), 7691−7696.
(36) Yang, J.; Yin, J.; Guo, Q.; Xie, C.; Yang, Q.; Kong, Z.; Kang, Z.; Wang, R.; Sun, D. Guest-induced proton conductivity of two-dimensional layered hydrogen-bonded organic frameworks. *Inorg. Chem. Front.* **2023**, *10* (21), 6262−6268.
(37) Tong, L.; Lin, Y.; Kou, X.; Shen, Y.; Shen, Y.; Huang, S.; Zhu, F.; Chen, G.; Ouyang, G. Pore-Environment-Dependent Photo-responsive Oxidase-Like Activity in Hydrogen-Bonded Organic Frameworks. *Angew. Chem. Int. Ed.* **2023**, *62* (13), No. e202218661.
(38) Zhang, H.; Yu, D.; Liu, S.; Liu, C.; Liu, Z.; Ren, J.; Qu, X. NIR-II Hydrogen-Bonded Organic Frameworks (HOFs) Used for Target-Specific Amyloid-β Photooxygenation in an Alzheimer's Disease Model. *Angew. Chem. Int. Ed.* **2022**, *61* (2), No. e202109068.
(39) Chen, G.; Huang, S.; Ma, X.; He, R.; Ouyang, G. Encapsulating and stabilizing enzymes using hydrogen-bonded organic frameworks. *Nat. Protoc.* **2023**, *18* (7), 2032−2050.
(40) Liu, S.; Sun, Y. Co-encapsulating Cofactor and Enzymes in Hydrogen-Bonded Organic Frameworks for Multienzyme Cascade Reactions with Cofactor Recycling. *Angew. Chem. Int. Ed.* **2023**, *62* (42), No. e202308562.
(41) Liang, W.; Carraro, F.; Solomon, M. B.; Bell, S. G.; Amenitsch, H.; Sumby, C. J.; White, N. G.; Falcaro, P.; Doonan, C. J. Enzyme Encapsulation in a Porous Hydrogen-Bonded Organic Framework. *J. Am. Chem. Soc.* **2019**, *141* (36), 14298−14305.
(42) Huang, Q.; Otake, K.-i.; Kitagawa, S. A Nitro-Modified Luminescent Hydrogen-Bonded Organic Framework for Non-Contact and High-Contrast Sensing of Aromatic Amines. *Angew. Chem. Int. Ed.* **2023**, *62* (43), No. e202310225.
(43) Chen, S.; Ju, Y.; Zhang, H.; Zou, Y.; Lin, S.; Li, Y.; Wang, S.; Ma, E.; Deng, W.; Xiang, S.; et al. Photo Responsive Electron and Proton Conductivity within a Hydrogen-Bonded Organic Framework. *Angew. Chem. Int. Ed.* **2023**, *62* (34), No. e202308418.
(44) Wang, C.; Song, X.; Wang, Y.; Xu, R.; Gao, X.; Shang, C.; Lei, P.; Zeng, Q.; Zhou, Y.; Chen, B.; et al. A Solution-Processable Porphyrin-Based Hydrogen-Bonded Organic Framework for Photo-electrochemical Sensing of Carbon Dioxide. *Angew. Chem. Int. Ed.* **2023**, *62* (43), No. e202311482.
(45) Wang, B.; He, R.; Xie, L.-H.; Lin, Z.-J.; Zhang, X.; Wang, J.; Huang, H.; Zhang, Z.; Schanze, K. S.; Zhang, J.; et al. Microporous Hydrogen-Bonded Organic Framework for Highly Efficient Turn-Up Fluorescent Sensing of Aniline. *J. Am. Chem. Soc.* **2020**, *142* (28), 12478−12485.
(46) Hisaki, I.; Nakagawa, S.; Ikenaka, N.; Imamura, Y.; Katouda, M.; Tashiro, M.; Tsuchida, H.; Ogoshi, T.; Sato, H.; Tohnai, N.; et al. A Series of Layered Assemblies of Hydrogen-Bonded, Hexagonal Networks of C_3-Symmetric π-Conjugated Molecules: A Potential Motif of Porous Organic Materials. *J. Am. Chem. Soc.* **2016**, *138* (20), 6617−6628.
(47) Wang, Y.; Ma, K.; Bai, J.; Xu, T.; Han, W.; Wang, C.; Chen, Z.; Kirlikovali, K. O.; Li, P.; Xiao, J.; et al. Chemically Engineered Porous Molecular Coatings as Reactive Oxygen Species Generators and Reservoirs for Long-Lasting Self-Cleaning Textiles. *Angew. Chem. Int. Ed.* **2022**, *61* (8), No. e202115956.
(48) Yin, Q.; Alexandrov, E. V.; Si, D.-H.; Huang, Q.-Q.; Fang, Z.-B.; Zhang, Y.; Zhang, A.-A.; Qin, W.-K.; Li, Y.-L.; Liu, T.-F.; et al. Metallization-Prompted Robust Porphyrin-Based Hydrogen-Bonded Organic Frameworks for Photocatalytic CO_2 Reduction. *Angew. Chem. Int. Ed.* **2022**, *61* (6), No. e202115854.
(49) Zhang, X.; Wang, J.-X.; Li, L.; Pei, J.; Krishna, R.; Wu, H.; Zhou, W.; Qian, G.; Chen, B.; Li, B. A Rod-Packing Hydrogen-Bonded Organic Framework with Suitable Pore Confinement for Benchmark Ethane/Ethylene Separation. *Angew. Chem. Int. Ed.* **2021**, *60* (18), 10304−10310.
(50) Yin, Q.; Li, Y.-L.; Li, L.; Lü, J.; Liu, T.-F.; Cao, R. Novel Hierarchical Meso-Microporous Hydrogen-Bonded Organic Framework for Selective Separation of Acetylene and Ethylene versus Methane. *ACS Appl. Mater. Interfaces* **2019**, *11* (19), 17823−17827.
(51) Wang, J.-X.; Gu, X.-W.; Lin, Y.-X.; Li, B.; Qian, G. A Novel Hydrogen-Bonded Organic Framework with Highly Permanent Porosity for Boosting Ethane/Ethylene Separation. *ACS Mater. Lett.* **2021**, *3* (5), 497−503.
(52) Yu, B.; Geng, S.; Wang, H.; Zhou, W.; Zhang, Z.; Chen, B.; Jiang, J. A Solid Transformation into Carboxyl Dimers Based on a Robust Hydrogen-Bonded Organic Framework for Propyne/Propylene Separation. *Angew. Chem. Int. Ed.* **2021**, *60* (49), 25942−25948.
(53) Gao, J.; Cai, Y.; Qian, X.; Liu, P.; Wu, H.; Zhou, W.; Liu, D.-X.; Li, L.; Lin, R.-B.; Chen, B. A Microporous Hydrogen-Bonded Organic Framework for the Efficient Capture and Purification of Propylene. *Angew. Chem. Int. Ed.* **2021**, *60* (37), 20400−20406.
(54) Yuan, Z.; Jiang, X.; Chen, L.; Chen, J.; Li, L.; Yang, Y.; Li, Y.; Xiang, F.; Xiang, S.; Chen, B.; et al. Sticked-Layer Strategy to a Flexible-Robust Hydrogen-Bonded Organic Framework for Efficient C_2H_2/CO_2 Separation. *CCS Chem.* **2023**, 1.
(55) Chen, Y.; Yang, Y.; Wang, Y.; Xiong, Q.; Yang, J.; Xiang, S.; Li, L.; Li, J.; Zhang, Z.; Chen, B. Ultramicroporous Hydrogen-Bonded Organic Framework Material with a Thermoregulatory Gating Effect for Record Propylene Separation. *J. Am. Chem. Soc.* **2022**, *144* (37), 17033−17040.
(56) Yang, Y.; Zhang, H.; Yuan, Z.; Wang, J.-Q.; Xiang, F.; Chen, L.; Wei, F.; Xiang, S.; Chen, B.; Zhang, Z. An Ultramicroporous Hydrogen-Bonded Organic Framework Exhibiting High C_2H_2/CO_2 Separation. *Angew. Chem. Int. Ed.* **2022**, *61* (43), No. e202207579.
(57) Zhang, H.; Li, Y.; Chen, L.; Yang, Y.; Lin, H.; Xiang, S.; Chen, B.; Zhang, Z. A crystalline and stable microporous framework based on the dative B←N bonds. *Chem.* **2023**, *9* (1), 242−252.
(58) Li, P.; He, Y.; Zhao, Y.; Weng, L.; Wang, H.; Krishna, R.; Wu, H.; Zhou, W.; O'Keeffe, M.; Han, Y.; et al. A Rod-Packing Microporous Hydrogen-Bonded Organic Framework for Highly Selective Separation of C_2H_2/CO_2 at Room Temperature. *Angew. Chem. Int. Ed.* **2015**, *54* (2), 574−577.
(59) Cai, Y.; Chen, H.; Liu, P.; Chen, J.; Xu, H.; Alshahrani, T.; Li, L.; Chen, B.; Gao, J. Robust microporous hydrogen−bonded organic framework for highly selective purification of methane from natural gas. *Microporous Mesoporous Mater.* **2023**, *352*, No. 112495.

https://doi.org/10.1021/cbe.3c00100
Chem Bio Eng. 2024, 1, 615−622

(60) Zentner, C. A.; Lai, H. W. H.; Greenfield, J. T.; Wiscons, R. A.; Zeller, M.; Campana, C. F.; Talu, O.; FitzGerald, S. A.; Rowsell, J. L. C. High surface area and Z′ in a thermally stable 8-fold polycatenated hydrogen-bonded framework. *Chem. Commun.* **2015**, *51* (58), 11642−11645.
(61) Pei, J.; Wen, H.-M.; Gu, X.-W.; Qian, Q.-L.; Yang, Y.; Cui, Y.; Li, B.; Chen, B.; Qian, G. Dense Packing of Acetylene in a Stable and Low-Cost Metal−Organic Framework for Efficient C_2H_2/CO_2 Separation. *Angew. Chem. Int. Ed.* **2021**, *60* (47), 25068−25074.
(62) Wang, H.; Li, B.; Wu, H.; Hu, T.-L.; Yao, Z.; Zhou, W.; Xiang, S.; Chen, B. A Flexible Microporous Hydrogen-Bonded Organic Framework for Gas Sorption and Separation. *J. Am. Chem. Soc.* **2015**, *137* (31), 9963−9970.
(63) Yin, Q.; Lü, J.; Li, H.-F.; Liu, T.-F.; Cao, R. Robust Microporous Porphyrin-Based Hydrogen-Bonded Organic Framework for Highly Selective Separation of C_2 Hydrocarbons versus Methane. *Cryst. Growth Des.* **2019**, *19* (7), 4157−4161.
(64) Zhou, Y.; Kan, L.; Eubank, J. F.; Li, G.; Zhang, L.; Liu, Y. Self-assembly of two robust 3D supramolecular organic frameworks from a geometrically non-planar molecule for high gas selectivity performance. *Chem. Sci.* **2019**, *10* (26), 6565−6571.

https://doi.org/10.1021/cbe.3c00100
Chem Bio Eng. 2024, 1, 615−622